Gautam Choubey* and K. M. Pandey

Numerical Studies on the Performance of Scramjet Combustor with Alternating Wedge-Shaped Strut Injector

DOI 10.1515/tjj-2015-0048
Received August 12, 2015; accepted August 27, 2015

Abstract: Numerical analysis of the supersonic combustion and flow structure through a scramjet engine at Mach 7 with alternating wedge fuel injection and with three angle of attack ($\alpha = -3°$, $\alpha = 0°$, $\alpha = 3°$) have been studied in the present research article. The configuration used here is slight modification of the Rabadan et al. scramjet model. Steady two dimensional (2D) Reynolds-averaged Navier-Stokes (RANS) simulation and Shear stress transport (SST) based on k–ω turbulent model is used to predict the shock structure and combustion phenomenon inside the scramjet combustor. All the simulations are done by using Ansys 14-Fluent code. The combustion model used here is the combination of eddy dissipation and finite rate chemistry models since this model avoids Arrhenius calculations in which reaction rates are controlled by turbulence. Present results show that the geometry with negative angle of attack ($\alpha = -3°$) have lowest ignition delay and it improves the performance of scramjet combustor as compared to geometry with $\alpha = 0°$, $\alpha = 3°$. The combustion phenomena and efficiency is also found to be stronger and highest in case of $\alpha = -3°$.

Keywords: scramjet, hypersonic combustion, k–ω SST model, flame holder, wedge-shaped strut injector

PACS® (2010). 47.27.E-, 47.70.Pq, 47.40.Ki

Introduction

The supersonic combustor ramjet (Scramjet) permits the course through the combustor to stay supersonic. The scramjet combustor is the most encouraging air breathing propulsive framework and fitting decision for hypersonic flight ($M > 5$). Numerous analysts are dealing with the advancement of the scramjet engine because of its applications in the military rockets, minimal effort space get to, and space tourism in particular. Computational analysis of scramjet combustor at flight Mach no 7 is done by Pandey et al. [1]. They found that the shock relocation inside the combustor improved the burning and diminished the ignition delay. Maier et al. [2] in their work revealed that supersonic ignition is a testing, complex procedure which incorporates numerous phenomena, for example, turbulent mixing in the middle of air and H_2, shock formation and heat discharge which is influenced by combustor geometry.

In order to accomplish effective burning [3], it is important to improve and quicken the mixing between the fuel and the air and also to decrease the pressure losses in the combustion. Rabadan et al. [4] chipped away at the three unique angle of attacks ($\alpha = -5°$, $\alpha = 0°$, $\alpha = 5°$) at flight Mach no.8 for two cases. For one situation without injector body and a case with a focal lobed strut injector and found that No impact of the focal strut injector in upstream course towards the isolator was discovered. The most minimal ignition postponement was enrolled for $\alpha = -5°$. He explored [5] numerically hydrogen-filled scramjet combustor at flight conditions and found that as the equivalence ratio was expanded, the ignition got to be more grounded bringing about an upstream uprooting of the shock train creating distinctive pressure varieties. Nguyen [6] took a shot at relaminarization in supersonic and hypersonic flows numerically and his discoveries are in the region downstream of the extension corner, the pressure and the wall shear stress are diminished and the boundary layer is more full and thicker. Aleksandrov et al. [7] demonstrated that little entrance of fuel into supersonic stream causes ignition just close to a wall, large losses of aggregate pressure. Skinner and Stalker [8] found that at lower pressure, the ignition postpones and heat discharge times will be much more prominent than the base estimations of 0.5 and 1 ms separately. Swithenbank [9] took a shot at hypersonic air-breathing impetus and his discoveries are concoction modification time for burning can be vast at low temperature and

***Corresponding author: Gautam Choubey,** Department of Mechanical Engineering, N.I.T Silchar, Assam, India, E-mail: gautam_dadaa@yahoo.com
K. M. Pandey, Department of Mechanical Engineering, N.I.T Silchar, Assam, India, E-mail: Kmpandey2001@yahoo.com

pressure. Momtchiloff et al. [10] demonstrated that the ignition delay length increments quickly at the lower flight Mach numbers. Oldenborg et al. [11] found that high Mach number flight additionally brings about short residence times (millisecond time range) in a hypersonic combustor which causes poor synthetic ignition productivity. Radhakrishnan et al. [12] found that the flame spread delivers a progression of diagonal shock waves that reignite the center stream, making a slanted explosion wave whose connection with the along the side growing limit layer fire offers ascend to a typical explosion wave that proliferates. Kumaran and Babu [13] researched of the impact of chemistry models on the numerical expectations of the supersonic burning of Hydrogen and their discoveries are multi-step chemistry predicts higher and more extensive spread heat discharge than what is anticipated by single step chemistry. Zakrzewski and Milton [14] did an examination on supersonic fluid fuel jets injected into air and demonstrated that supersonic fluid jets $M = 1.8$ creates from a flat front to an adjusted bow inside of by most accounts 10 mm $M = 5.2$, the bow shape is more pointed and hints at a wavering from additional to less pointed. Kyung Moo Kim et al. [15] introduced numerical study on supersonic combustion with cavity based fuel infusion and discovered when the wall angle of cavity increases, the ignition proficiency is enhanced, yet total pressure loss increased. Cecere and Ingenito [16] took a shot at Hydrogen/air supersonic combustion phenomena for future hypersonic vehicles and their discoveries are the heat discharged and the quick hydrogen jet creates 3-D huge structures and expansive vorticity rates, in this manner improving turbulent mixing. Tchuen [17] found that Real gas impacts altogether change the stream field behind the shock wave. Deepu [18] completed recent advances in experimental and numerical analysis of scramjet combustor flow fields and found that increase in jet to free stream force flux proportion will bring about the increment of jet infiltration to free stream for a wide range of jets. Contingent upon the measure of injected fuel, it is conceivable to change from one combustion mode to another [19]. Ramp and strut injectors have been studied previously and it was observed that they enhance the turbulent mixing in a rectangular unique supersonic ignition chamber [20]. At the point when the measure of the injected fuel is small, a lean combustion happens, expanding the measure of fuel prompts solid ignition. Lean combustion is described by low heat discharge and solid ignition by an arrangement of numerous shocks with a subsequent substantial pressure rise. Notwithstanding, a lot of fuel can prompt heat gagging brought on by the substantial heat discharged in the combustion chamber. Aso et al. [21] took a shot at principal investigation of supersonic burning in immaculate wind current with utilization of shock passage and their discoveries are, the increment of injection pressure produced solid bow shock, bringing about the pressure loses. The shock generator is a compelling system to quicken the combustion. The increment of the injection aggregate pressure raises the entrance of fuel; therefore, the reaction zone grows to the focal point of stream field.

The aim of the present work is to investigate numerically the flow phenomena in scramjet combustors for different design conditions by modifying the scramjet model which is used by Rabadan et al. The presence of three angle of attack ($\alpha = -3°$, $\alpha = 0°$, $\alpha = 3°$) and its impact on the performance of scramjet combustor is presented in this paper. The effect of shocks generated by different geometry on combustion efficiency is also reported. It is found that modified scramjet combustors with negative angle of attack ($\alpha = -3°$) have improved the combustion efficiency and decreased the ignition delay.

Mathematical and numerical modeling

The advantage of employing the complete Navier-Stokes equations extends not only the investigations that can be carried out on a wide range of flight conditions and geometries, but also in the process the location of shock wave, as well as the physical characteristics of the shock layer, can be precisely determined. We begin by describing the two-dimensional forms of the Navier-Stokes equations below.

Mass conservation (Continuity equation)

$$\frac{\partial \rho}{\partial t} + \frac{\partial}{\partial x_i}(\rho u_i) = 0 \quad i = 1, 2 \tag{1}$$

Momentum conservation

$$\frac{\partial}{\partial t}(\rho u_i) + \frac{\partial}{\partial x_i}(\rho u_i u_j) = -\frac{\partial P}{\partial x_i} + \frac{\partial}{\partial x_i}(\tau_{ij}) \quad i, j = 1, 2 \tag{2}$$

Energy conservation

$$\frac{\partial}{\partial t}(\rho e_t) + \frac{\partial}{\partial x_i}(\rho h_t u_i) = \frac{\partial}{\partial x_i}(\tau_{ij} u_i - q_i) \quad i, j = 1, 2 \tag{3}$$

Transport equations for the SST k–ω model

The turbulence kinetic energy, k, and the specific dissipation rate, ω are obtained from the following transport equations:

$$\frac{\partial}{\partial x_i}(\rho k u_i) = \frac{\partial}{\partial x_j}\left(\Gamma_k \frac{\partial k}{\partial x_j}\right) + \tilde{G}_k - Y_k + S_k \tag{4}$$

where $i = 1, 2$ and $j = 1, 2$

$$\text{Again } \frac{\partial}{\partial x_i}(\rho \omega u_i) = \frac{\partial}{\partial x_j}\left(\Gamma_\omega \frac{\partial \omega}{\partial x_j}\right) + G_\omega - Y_\omega + D_\omega + S_\omega \tag{5}$$

where $i = 1, 2$ and $j = 1, 2$

where $\tilde{G}_k$ represents the generation of turbulent kinetic energy due to mean velocity gradients G_ω represents the generation of ω. Γ_k And Γ_ω represent the effective diffusivity of k and ω respectively. Y_k And Y_ω represent the dissipation of k and ω due to turbulence. D_ω represents the cross-diffusion term, calculated as described below. S_k And S_ω are user-defined source terms.

Cross-diffusion modification

The SST $k-\omega$ model is based on both the standard $k-\omega$ model and the standard $k-\varepsilon$ model. To blend these two models together, the standard $k-\varepsilon$ model has been transformed into equations based on k and ω, which leads to the introduction of a cross-diffusion term. D_ω is defined as

$$D_\omega = 2(1-F_1)\rho\sigma_{\omega,2}\frac{1}{\omega}\frac{\partial k}{\partial x_j}\frac{\partial \omega}{\partial x_j} \tag{6}$$

Model constants

$$\sigma_{k,1} = 1.176, \sigma_{\omega,1} = 2.0, \sigma_{k,2} = 1.0, \sigma_{\omega,2} = 1.168,$$
$$\alpha_1 = 0.31, \beta_{i,1} = 0.075, \beta_{i,2} = 0.0828$$

Species transport equation

$$\frac{\partial}{\partial t}(\rho Y_n) + \frac{\partial}{\partial x_i}(\rho Y_n u_i) = \frac{\partial}{\partial x_i}\left(-\vec{J}_i\right) + \omega_n \quad i = 1, 2 \tag{7}$$

Combustion modeling

The most common combustion modeling angle of attack and also one used in this work is the combination of finite rate-eddy dissipation model. It is based on the assumption that chemical reactions are fast relative to the transport processes of the flow. Single step chemistry model is taken to find the flow physics phenomenon inside the combustor at hypersonic condition. The reaction used for the Scramjet was the hydrogen-water reaction:

$$2H_2 + O_2 = 2H_2O$$

Flow modeling and simulation

The geometry and model used here is same as that of Rabadan et al. [4] for $\alpha = 0°$ angle of attack. For negative and positive angle of attack slight modification is done in the geometry which is completely different than that of Rabadan et al. [4]. The expansion of preheated air takes place through a compression ramps which then enters in to combustion section at $M = 7$. The compression ramp section has a width of 65 mm and a height of 122 mm at the entrance. A divergence angle of 8° is provided on the compression ramp of the combustor which has a total length of 487 mm. The wedge shaped strut of 86 mm long, 65 mm width and 7 mm height is placed in the combustor chamber at a distance of 650 mm from the inlet. Hydrogen fuel (H_2) is injected parallel to the air stream at $M = 2$ through a row of 7 horizontal and 6 vertical injection ports of the strut each with an area of 5.25 mm^2 and 1.20 mm^2 mm respectively in trailing edge. The total length of the scramjet is 1,550 mm with a constant cross-section width of 65 mm and maximum height of 71 mm at the exit (Figures 1 and 2).

Hydrogen is injected parallel to the stream and mixed down-stream by method for strong stream wise vortices delivered by the geometry of the wedge shaped strut injector. The boundary conditions for the present case (Air $M = 7$, Hydrogen $M = 2$) is demonstrated in Table 1 which is completely different as used by Rabadan et al. [4]. In the present work, we used different boundary conditions. For all computational analysis, wall temperatures were assumed to be Twall = 750 K since wall cooling is normal in a real flight. Hydrogen was injected at the static temperature of $TH_2 = 350$ K with a Mach number of $M = 2$. To diminish the computational time as much as could be expected under the circumstances, yet at the same time holding every single significant physic of the scramjet combustor, the computational setup is streamlined as in, all the grids, displaying and computational investigations are done in 2D. In the present case all the 2D models and grids are generated utilizing ICEM-CFD [22] and computational investigation are finished by utilizing Ansys 14-Fluent code [22] (Figure 3).

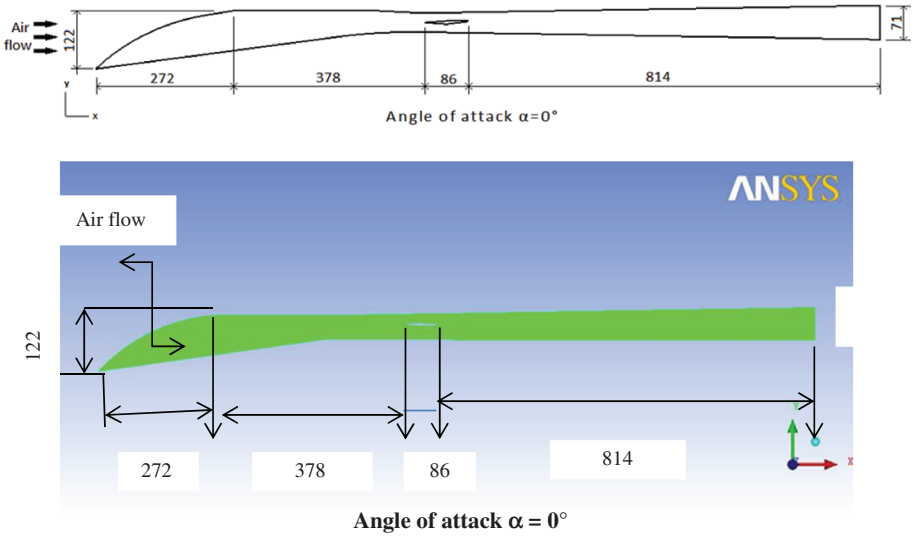

Figure 1: General dimensions of the inlet-combustor configuration with wedge shaped strut injector (all dimensions are in mm). Angle of attack $\alpha = 0$ is defined with the parallel position of the wedge shaped injector with respect to the incoming free stream flow [4].

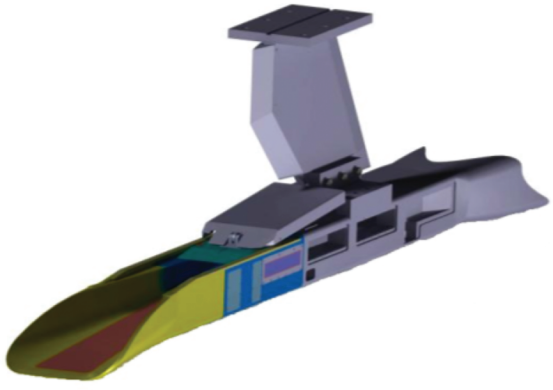

Figure 2: Scramjet Hypersonic test model [4].

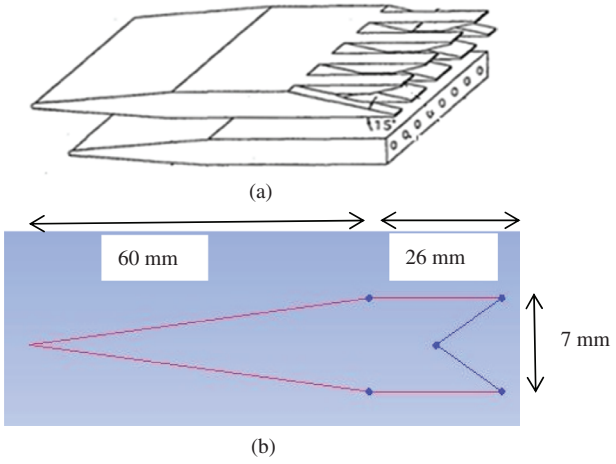

Figure 3: Strut with alternating wedge injector (a) in 3D and (b) 2D.

Table 1: Inflow conditions of the incoming air stream and hydrogen jet for air Mach number 7 and H_2 Mach number 2.

S. No	Variables	Air	Hydrogen
1	*M*	7	2
2	T(k)	530	300
3	P(Pa)	20,000	20,000
4	U(m/s)	925.25	1318.76
5	Y_{O2}	0.232	0
6	Y_{N2}	0.736	0
7	Y_{H2O}	0.032	0
8	Y_{H2}	0	1

Grid generation

For Strut with wedge-shaped injectors computational grids were generated. 2D, unstructured quadrilateral grids are generated using ICEM-CFD [22]. Numerical figuring of the stream was initially done on a base framework with 130,542 components individually. After refinement a framework with 272,136 components for wedge shaped strut injector have been taken as final grid for every single consequent computation. Figure 4 shows the mesh generation in details.

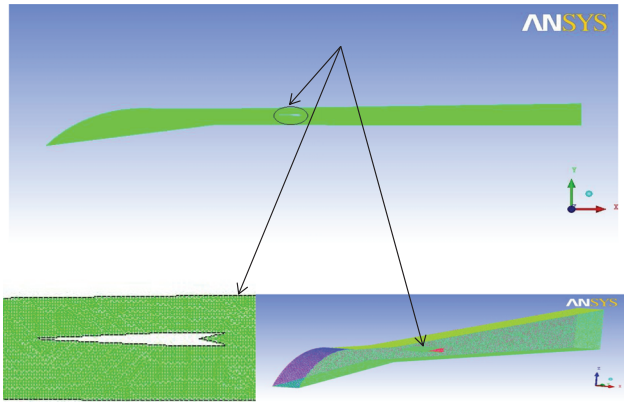

Figure 4: Grid generation around the strut injector with wedge inlet 2D and 3D.

Grid convergence test

Grid convergence is the term used to depict minimization of the lapse and change of results by utilizing progressively smaller grid sizes for figuring. A calculation should approach the correct answer as the mesh becomes finer; hence the term grid convergence comes to picture Grid convergence Test is completed here to analyze the effect of grid number on the maximum static temperature of the stream field

As illustrated from Figure 5 a good result is observed between 272,136 elements and 302,678 elements. Hence the current analysis is carried out using a minimum grid size of 272,136 elements.

Boundary conditions

Three sorts of boundaries are connected: inflow, surge and settled walls and the whole stream field is thought to be supersonic. Dirichlet limit conditions are connected for variables at inflow and Neumann limit conditions are utilized for all variables at surge. Likewise no slip condition is applied on fixed walls.

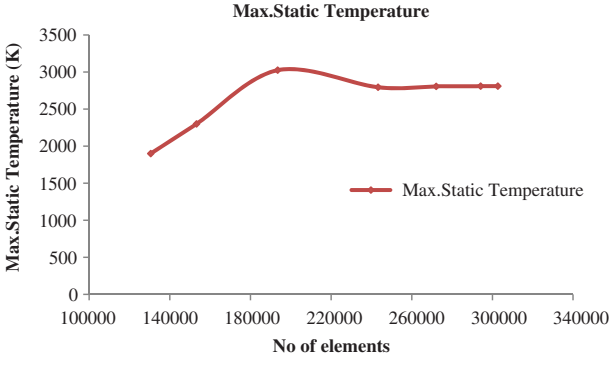

Figure 5: Grid Independence Test for the strut with wedge inlet.

Approximations and idealization

- The flow is considered to be in steady state.
- The flow is assumed to be two-dimensional.
- The k–ω SST model is taken into consideration.
- The gas is compressible and obeying the ideal gas laws.

For all simulations, wall temperatures were set to Twall = 750 K.

Results and discussions

Flow field phenomena in Scramjet combustors for different geometry ($\alpha = -3°$, $\alpha = 0°$, $\alpha = 3°$) are studied numerically and reported. The formation of shock wave by wedge strut and its effects on ignition delay of different design of scramjet and on combustion efficiency are also reported.

Figure 6 demonstrates temperature distribution for the investigated angles of attack. The heat expansion in the combustor changes both the static temperature and the stream speed. In this way, it is reflected in an increment of aggregate temperature. When hydrogen is injected through the wedge strut, at that very moment it starts mixing with the incoming air. After hydrogen is mixed, pressure and temperature are sufficiently high for auto ignition, then burning begins.

The power of the vortices depends principally on the injector's geometry. The ignition delay is influenced by the variation of the angle of attack. The ignition delay is estimated from the computations using an absolute temperature value. The absolute temperature, rather than pressure, is employed because it is a more sensitive parameter in the computations. Here we assumed 2,000 K temperature as the base temperature for ignition delay calculation that means the geometry which reaches the 2,000 K temperature earlier have lowest ignition delay and here the ignition delay is measured in mm. Hence the shortest ignition delay is found for the arrangement with $\alpha = -3°$ while the longest ignition delay shows up for $\alpha = 3°$. The highest temperature is observed for a negative angle of attack $\alpha = -3°$

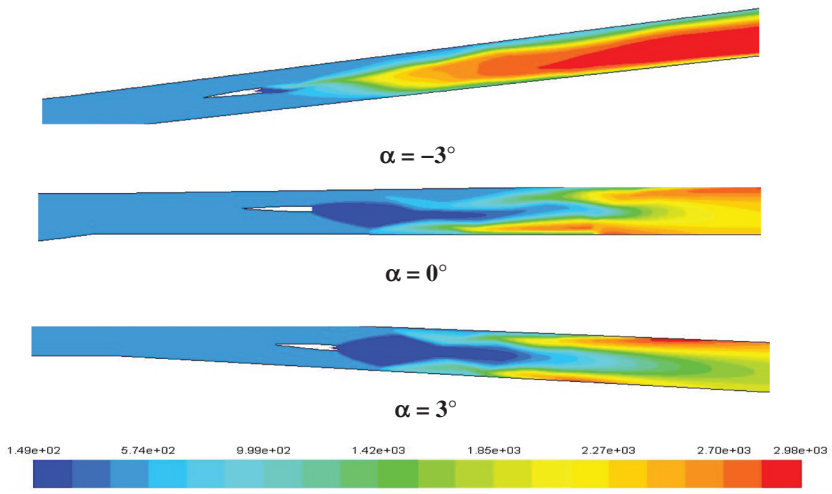

Figure 6: Temperature distribution for different angles of attack [α = –3°, $\alpha = 0°$, $\alpha = 3°$] for $M = 7$.

approximately Tmax = 2,980 K and the sudden increment in temperature happens approximately 95 mm downstream of the fuel injection. For the setup with $\alpha = 0°$, $\alpha = 3°$ the ignition delay is roughly 180 mm and 410 mm.

In case of Mach no contour (Figure 7) we can see that oblique shocks are formed at the tip of the wedge strut for three angle of attack configuration. Due to these reflected shock waves from the combustor wall, wall temperature increases which is then followed by the formation of subsonic recirculation zone at the base of the wedge which will help in stabilizing the flame during combustion process. Figure 7(a) also shows variation of the Mach number

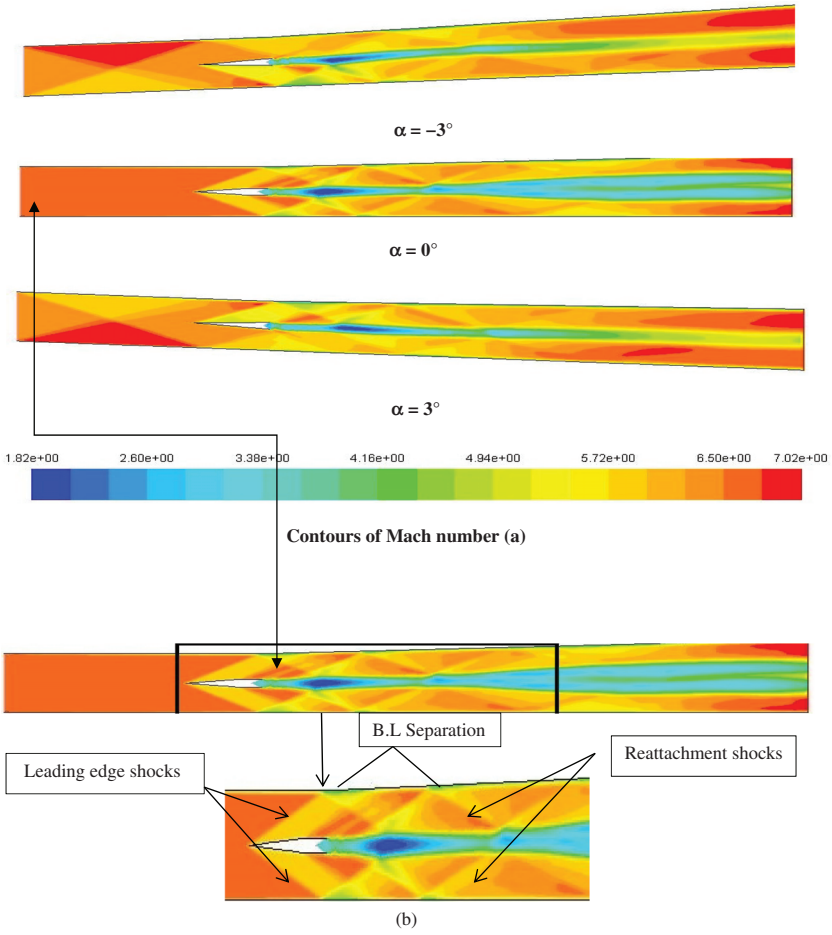

Figure 7: (a) Computed Mach number distribution for different angles of attack (α) for $M = 7$ and (b) enlarged version of contour plots of Mach number for $\alpha = 0°$.

for three different geometries of scramjet combustor at the different level, at the entrance the air Mach no is 7, at the base of the wedge strut the hydrogen is injected at Mach no 2. For $\alpha = -3°$and $\alpha = 0°$, a subsonic area is found at the compression where the pressure shock always at the top wall. For all the geometries, in the middle of the chamber the Mach number values are reduced to below 2 due to heat release in the combustion process which actually decelerate the flow. The enlarged version of contour plots of Mach number for $\alpha = 0°$ is shown in Figure 7(b).

Figure 8(a) shows the enlarged version of shock waves interactions by using contour plots of density for $\alpha = 0°$ whereas Figure 8(b) represents the contours of density for different angle of attack. Here also with H_2 injection, oblique shocks are shaped at the tip of the wedge that is later reflected by the upper and lower walls. At the upper and lower walls, the boundary layer is influenced by the reflected sideways shocks. In a few places the reflected shock waves are avoided by the hydrogen jets. The boundary layer on the wedge surface isolates at the base and a shear layer is framed. This shear layer is normally unsteady and is consequently inclined to break-up. Because of the one-sided divergent channel the upper reflecting shock hits the H_2 filled wake further downstream than the lower shock. In a few places the reflected shock waves are diverted by the hydrogen jets. After some separation the stream in the wake of the wedge is accelerated back to supersonic speed. A little triangular recirculation locale is framed simply behind the wedge brought about by low speed.

Figure 9 represents the contour of static pressure for three angle of attack configuration. Here at the main edge of the wedge strut injector, a shock is framed. This shock voyages downstream and is redirected at the top and base wall. The shock loses its intensity as its ventures towards the outlet.

Figure 10 represents the wall pressure distribution for different angle of attack. It is clear from the pressure distribution that the shock train turns out to be longer because of the higher number of the reflected shocks which are produced downstream of the strut injector. This prompts a further stream increasing speed in the unique piece of the combustor. The main edge shocks created upstream of the wedge injector are in charge of that conduct which comes about because of the high reflection points and in this way the little separations between the reflected shocks. This can be seen from

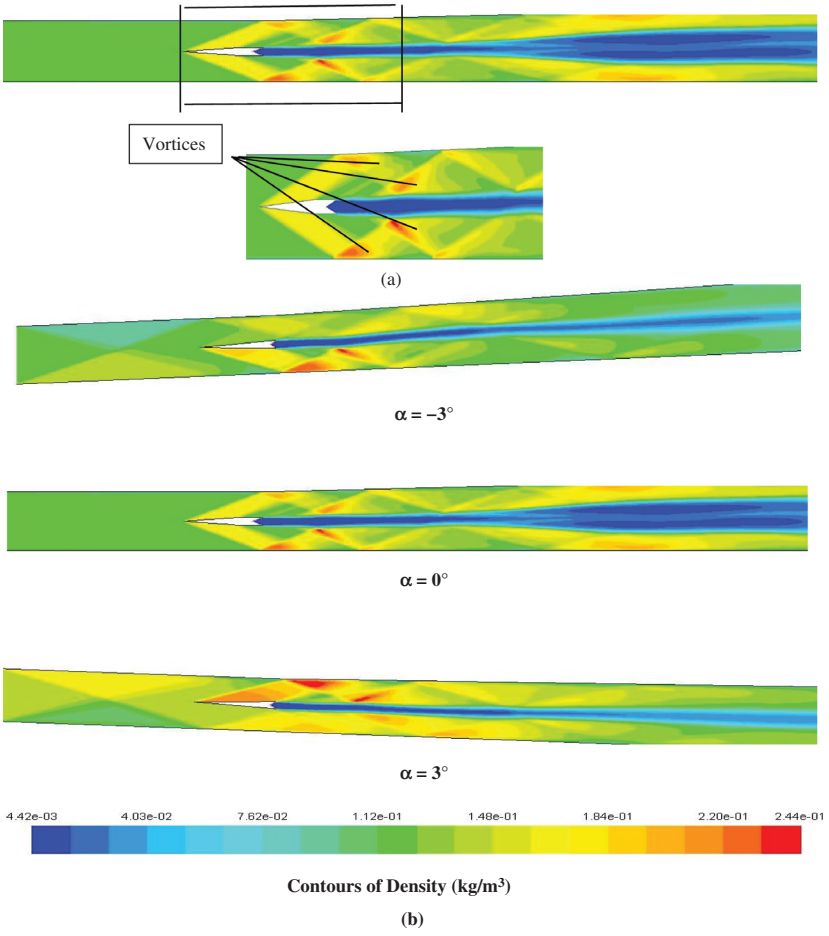

Figure 8: (a) CFD predicted enlarged version of shock waves interactions by using contour plots of density for $\alpha = 0°$ and (b) Density distribution for different angles of attack [$\alpha = -3°$, $\alpha = 0°$, $\alpha = 3°$] for $M = 7$.

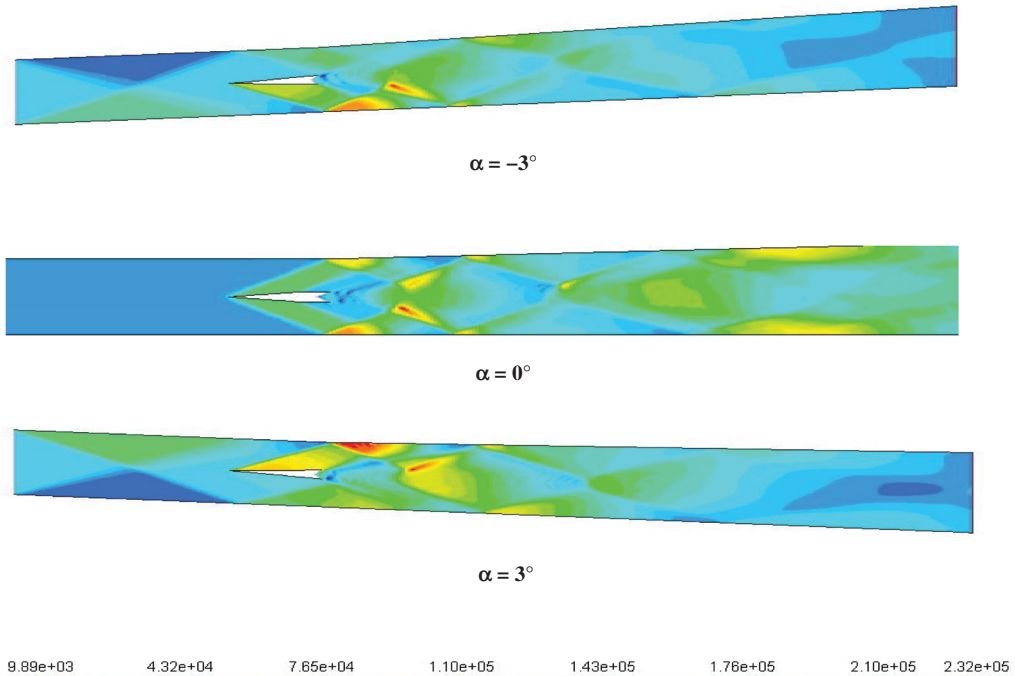

Figure 9: Pressure distribution for [$\alpha = 0°$] angle of attack for $M = 7$.

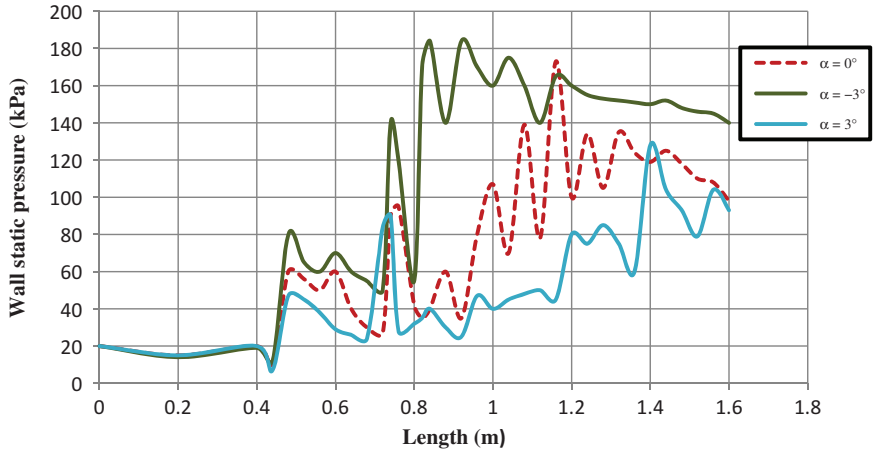

Figure 10: Computed wall pressure distribution at the top wall for different angles of attack. [$M = 7$].

Mach number contour plots which demonstrate the highly turbulent mixing region with high degree of vortex formation. The wedge-shaped injector changes the shock pattern and the stream properties by the development of a shock at its driving edge. For all cases, an upstream displacement of the shock train for a negative angle of attack is observed. At the point when ignition happens, the pattern of the wall pressure distribution changes. The heat expansion at supersonic speed produces pressure waves that proliferate and compress the stream outside the flame.

The highest pressure peak at the top wall is found at approximately $X = 845$ mm, $X = 940$ mm, with a corresponding pressure $p = 180$ kPa. This maximum value is observed for $\alpha = -3°$.

Combustion efficiency

The performance of the combustor is measured by combustion efficiency (η_c) [20] which is defined as

$$\eta_{comb}(x) = 1 - \frac{\int (A(x))\rho_{gas} u Y_{H_2} dA}{m_{\dot{H}_{2_{inj}}}}$$

where ρ is the gas density, Y_{H2} is the mass fraction of hydrogen, m_{H2inj} is the injected hydrogen mass flux, and u is the velocity component normal to the cross section. The combustion efficiency is presented in Figure 11. The plot begins directly after the trailing edge of the substituting wedge shaped injector ($x = 732$ mm) since no hydrogen is accessible in upstream course. The ignition of the fuel-air mixing happens downstream of the trailing edge of the injector. The combustion efficiency becomes close to the injection area where hydrogen is quickly mixed because of the stream wise vorticity. For the present case, the most astounding combustion efficiency for a stoichiometric condition ($ø = 1$) is around 80%. The high equivalence ratio and the high angle of attacking Mach number, prevents the total mixing of the fuel and oxidizer [4]. Combustion can't happen until miniaturized scale mixing has happened. For $ø = 1$, a lot of hydrogen is injected and not totally mixed. Thus, the ignition effectiveness diminishes. The strong vorticity delivered by the wedge formed injector is in charge of the mixing. As the vortices travel downstream they get to be frail and their capacity to spread the fuel into the encompassing stream diminish. This prompts a reduction in mixing and hence in combustion effectiveness.

In this case, Combustion efficiency reaches approximately 84% at a distance 1.2 m and then comes to 82% at 1.55 m and is maximum for $\alpha = -3°$ whereas for $\alpha = 0°$, $\alpha = 3°$ combustion efficiency reaches approximately 72% and 67%, respectively.

Mixing efficiency

Here hydrogen is transported and mixed by the vortices as they travel downstream in the center stream. In the close field of the infusion ports, hydrogen is mixed faster

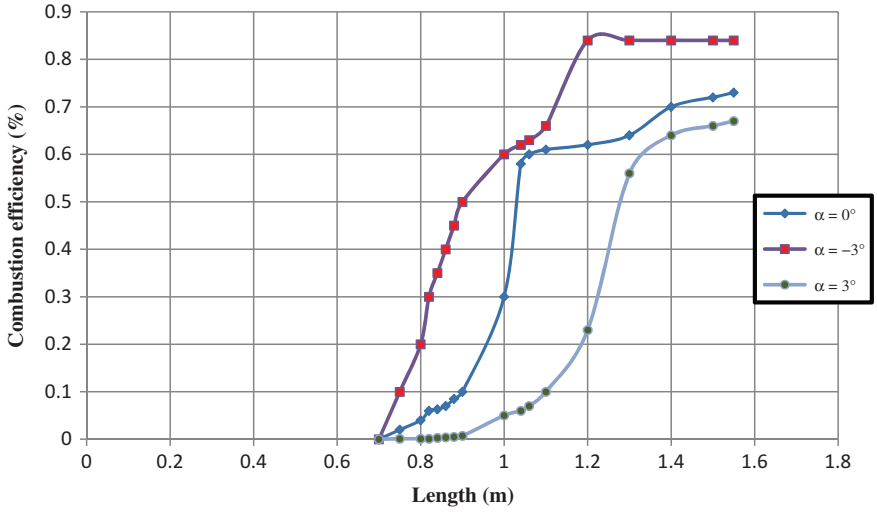

Figure 11: Computed combustion efficiency for different angles of attack [$M = 7$].

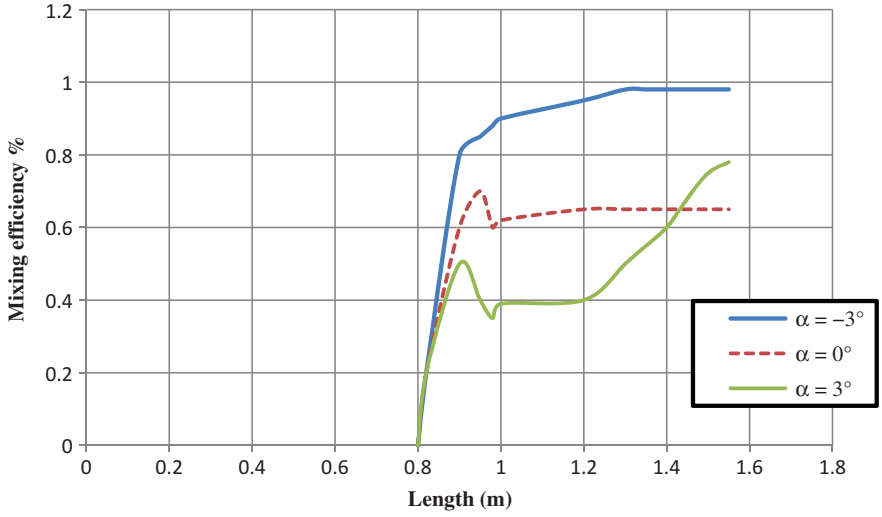

Figure 12: Computed mixing efficiency for different angles of attack. [$M = 7$] for wedge shaped strut injector.

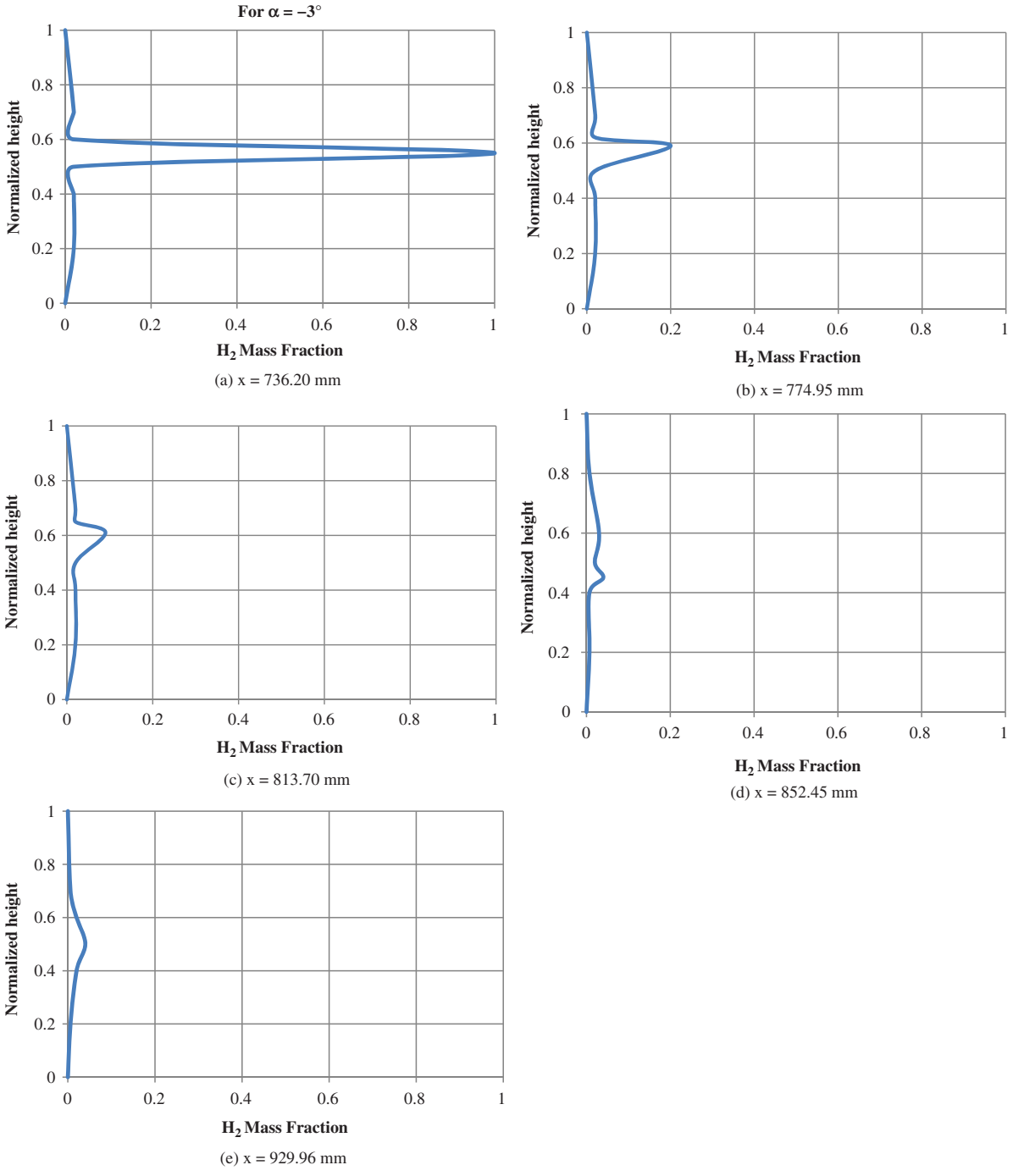

Figure 13: Computed Y_{H_2} for $\alpha = -3°$, for different axial locations at the symmetry plane.

because of the intensity of the vortices. As the vortices travel downstream, they get to be feeble and some measure of hydrogen still stays unmixed in their axis of rotation. This can be found in Figure 12 where the mixing effectiveness along the combustor length is plotted.

The distribution of the hydrogen mass fraction (Y_{H2}) at different axial locations is showed in Figure 13. The height is normalized with respect to the height of the local cross section. The cross section at five different axial locations for $\alpha = -3°$ is presented.

The distribution of the hydrogen mass fraction (Y_{H2}) at different axial locations at $x = 736.20$ mm and $x = 774.95$ mm.

The distribution of the hydrogen mass fraction (Y_{H2}) at different axial locations at $x = 813.70$ mm and $x = 852.45$ mm.

The distribution of the hydrogen mass fraction (Y_{H2}) at different axial locations at $x = 929.96$ mm.

Conclusions

The different flow phenomena and performance parameters such as static wall pressure, temperature, Mach number, density distribution and mass fraction of H_2O as well as combustion efficiency in scramjet combustors with different geometric configurations i.e. with three angle of attack ($\alpha = -3°\alpha = 0°$, $\alpha = 3°$) at air Mach no 7 were investigated numerically and reported in this study. K–ω SST turbulence model with the finite rate/eddy-dissipation reaction model and single-step chemistry model are employed to simulate the hypersonic flow field of the hydrogen fuelled scramjet combustor with three different types of geometries and the following conclusions are drawn at the basis of numerical results:

1. There is no impact of the wedge formed strut injector in upstream course towards the isolator was found as in.
2. The flow properties, shock structure, mixing and combustion phenomena are exceptionally sensible to the variation of the angle of attack. Here there is a displacement of the shock train in the upstream direction for a negative angle of attack was found. This shock displacement improved the combustion phenomena and decreased the ignition delay. This shock also helps in modifying the shock pattern in the combustor.
3. Here also, no thermal choking was found like that of the central lobed strut injector of Ramadan et al. For this setup, the range increment in the different combustor is adequate to keep away from inlet instabilities.
4. The most elevated temperature is enlisted for a negative angle of attack $\alpha = -3°$ approximately Tmax = 2,980 K. The least ignition delay was enlisted for ($\alpha = -3°$) more or less 95 mm downstream the hydrogen injection and longest ignition delay was found for positive angle of attack ($\alpha = 3°$).The combustion efficiency gives the best execute for $\alpha = -3°$.

Nomenclature

Symbol	Description/Definition	Unit
A	cross section area	m^2
f	fuel-air ratio, dimensionless	–
k	Turbulent kinetic energy	m^2/s^2
m°	Mass flow rate	kg/s
M	Mach number, dimensionless	–
P	Pressure,	Pa
T	Temperature	K
u	Axial velocity	m/s
x	Axial distance	mm
Y	Mass fraction, dimensionless	–
α	Angle of attack	degrees
ω	Specific turbulent dissipation rate	1/s
η	Efficiency parameter, dimensionless	–
ø	Equivalence ratio, dimensionless	–

Subscript	Description/Definition	Unit
comb	combustion	–
H_2	hydrogen	–
inj	injection	–
st	stoichiometric	–

References

1. Pandey KM, Roga S, Choubey G. Computational analysis of hypersonic combustor using strut injector at flight mach 7. Combust Sci Technol 2015;187:1392–407. DOI: 10.1080/00102202.2015.1035371.
2. Maier D, Kirstein S, Fuhrmann T, Denis SR, Hupfer A, Kau HP. Scramjet research activities at the institute of flight propulsion of the Techniche Unversitaet Muenchen, in: The 6th European Symposium on Aerothermodynamics for speed Vehicles, Versailles, France, 3–6 November, 2008.
3. Pandey KM, Sivasakthivel T. CFD analysis of mixing and combustion of a scramjet combustor with a planer strut injector. Int J Environ Sci Dev 2011;2:102–8.
4. Edder Rabadan Santana, Bernhard Weigand, "Numerical Investigation of Inlet Combustor Interactions for a Scramjet Hydrogen-Fueled Engine at a Flight Mach Number of 8" 18th AIAA/3AF International Space Planes and Hypersonic Systems and Technologies Conference, Tours, France, 2012. Paper ID AIAA-2012-5926, DOI: 10.2514/6.2012-5926
5. Rabadan E, Weigand B. Numerical Investigation of a Hydrogen-fueled Scramjet Combustor at Flight Conditions, EUCASS Book Series: Progress in Propulsion Physics, Volume 4, 373–394, ISBN 978-2-7598-0876-2, 2013
6. Nguyen T. Numerical Investigations of Relaminarization in Supersonic and Hypersonic Flows. Ph.D. Dissertation, Chair for Computational Analysis of Technical Systems, RWTH Aachen University, Aachen, Germany, to be published.
7. Yu V, Aleksandrov Alexander N, Prokhorov Vyacheslav LS. "Hypersonic Technology Development Concerning High Speed Air-Breathing Engines" Proceedings of ICFD 10th International

Congress of Fluid Dynamics, StellaDi Mare Sea Club Hotel, Ain Soukhna, Red Sea, Egypt. December 16–19, 2010.
8. Skinner KA, Stalker RJ. Species measurements in a hypersonic, hydrogen-air, combustion wake. Combust Flame 1996;106:478–86.
9. Swithenbank J. Hypersonic air-breathing propulsion In: Progress in aeronautical sciences 1967;7:229–94.
10. Momtchiloff IN, Taback ED, Buswell RF. Kinetics in hydrogen-air flow systems. I. Calculation of ignition delays for hypersonic ramjets. Symp Int Combust 1963;9:220–30.
11. Oldenborg RC, Harradine DM, Loge G, Lyman JL, Schott GL, Winn KR. Critical reaction rates in hypersonic combustion chemistry" Presented at the American Chemical Society national meeting, Miami, FL, September 10–15. Report no, LA-UR-89-2170, Los Alamos National Laboratory, 1989.
12. Yungster S, Radhakrishnan K. "Simulation of unsteady hypersonic combustion around projectiles in an expansion tube" vol. 11, Institute for Computational Mechanics in Propulsion, NASA Glenn Research Center, Cleveland, OH, 2001:1–12.
13. Kumaran K, Babu V. Investigation of the effect of chemistry models on the numerical predictions of the supersonic combustion of hydrogen. Combust Flame 2009;156:826–41.
14. Zakrzewski S, Milton. Supersonic liquid fuel jets injected into quiescent air. Int J Heat Fluid Flow 2004;25:833–40.
15. Kim KM, Baek SW, Han CY. Numerical study on supersonic combustion with cavity-based fuel injection. Int J Heat Mass Transfer 2004;47:271–86.
16. Cecere D, Ingenito A, Giacomazzi E, Romagnosi L, Bruno C. Hydrogen/air supersonic combustion for future hypersonic vehicles. Int J Hydrogen Energy 2011;36:11969–84.
17. Tchuen G, Burtschell Y, Zeitoun DE. Numerical study of the interaction of type IVr around a double-wedge in hypersonic flow. Comput Fluids Nov 2011;50:147–54.
18. Deepu M. Recent advances in experimental and numerical analysis of scramjet combustor flow fields. Inst Eng India (IE-I) May 2007;88:13–23.
19. Scheuermann T, Chun J, von Wolfersdorf J. Experimental investigations of scramjet combustor characteristics. 15th AIAA Space Planes and Hypersonic Systems and Technologies Conference (International), 2008.
20. Gerlinger P, Stoll P, Kindler M, Schneider F, Aigner M. Numerical investigation of mixing and combustion enhancement in supersonic combustors by strut induced stream wise vorticity. Aerosp Sci Technol 2008;12:159–68.
21. Aso S, Hakim AN, Miyamoto S, Inoue K, Tani Y. Fundamental study of supersonic combustion in pure air flow with use of shock tunnel. Acta Astronaut 2005;57:384–9.
22. ANSYS. ANSYS Fluent 14.0 theory guide, Canonsburg, PA 15317, ANSYS, Inc. 2011.